

Deuteron yields from LHC: Continuum correlations and in-medium effects

Benjamin Dönigus

*Institut für Kernphysik, Goethe Universität Frankfurt,
Max-von-Laue-Str. 1, 60438 Frankfurt am Main, Germany*

Gerd Röpke

*ExtreMe Matter Institute EMMI,
GSI Helmholtzzentrum für Schwerionenforschung,
Planckstrasse 1, 64291 Darmstadt, Germany
and
Institut für Physik, Universität Rostock,
18051 Rostock, Germany*

David Blaschke

*Institute of Theoretical Physics, University of Wrocław,
Max Born place 9, 50-204 Wrocław, Poland
(Dated: June 22, 2022)*

To explain the production of light nuclei in heavy-ion collisions at extreme energies, we focus on the deuteron case. A Gibbs ensemble at chemical freeze-out is a prerequisite to investigate the non-equilibrium evolution of the expanding fireball. Quantum statistical approaches allow to describe correlations including bound state formation in the strongly interacting and hot system. We consider the virial approach to evaluate proton-neutron correlations. In generalization of the treatment of protons in pionic matter (pion-proton puzzle), the influence of the pion environment on deuteron-like correlations is evaluated using data for the pion-deuteron scattering phase shifts. Calculated yields for deuteron production are compared with the ones observed at the LHC.

I. INTRODUCTION

Heavy-ion collisions (HICs) at the Large Hadron Collider (LHC) at CERN produce matter and antimatter with extreme concentration of energy, in a so-called fireball, at mid rapidity shortly after collision. Properties (e.g. composition, momentum distribution of components, etc.) of this extreme matter are reconstructed from measured yields, transverse-momentum spectra and correlations [1–17]. The production yields of composite particles, i.e. light (anti-)(hyper-)nuclei, in Pb-Pb collisions are very successfully explained by thermal [15, 18, 19] and coalescence models [17, 20–37]. There, thermodynamic equilibrium is assumed at freeze-out, and this determines a primordial distribution of the components of hot and dense matter. A simple statistical-thermal model, the hadron resonance gas model [18, 19, 38–43] has been used to describe the general features of the particle yields (including nuclei) from the fireball produced in central HIC, but cannot reproduce some details. Recent experiments deliver data with high precision and small statistical fluctuations so that more details of the HIC process are visible.

A first objection with respect to the use of the thermal model is that a HIC is a non-equilibrium process. Also if we assume local thermodynamic equilibrium, the parameters density n_C of conserved quantum number C , temperature T , and mean velocity \mathbf{v} of matter are depending on position and time. A hydrodynamical model may provide us with a profile $n_C(\mathbf{r}, t)$, $\mathbf{v}(\mathbf{r}, t)$, $T(\mathbf{r}, t)$ evolving in space and time. In this semi-empirical approach, at

a certain freeze-out time, the distribution functions remain fixed up to observation of particles by detectors. Alternatively, kinetic equations have been worked out, for instance quantum molecular dynamics, to describe the time evolution of the fireball. There, the inclusion of quantum correlations can only be done semi-empirically after a quasiparticle approach has been performed, for instance using a coalescence model.

A fundamental approach to the time evolution is given by the non-equilibrium statistical operator $\rho(t)$. According to the method of non-equilibrium statistical operator [44] it can be constructed from a relevant distribution $\rho_{\text{rel}}(t)$,

$$\rho(t) = \lim_{\epsilon \rightarrow 0} \epsilon \int_{-\infty}^t dt' e^{-\epsilon(t-t')} e^{-\frac{i}{\hbar} H(t-t')} \rho_{\text{rel}}(t') e^{\frac{i}{\hbar} H(t-t')} \quad (1)$$

which is a solution of the von Neumann equation. The choice of $\rho_{\text{rel}}(t)$ depends on the information necessary to describe the non-equilibrium state. An application of the Zubarev approach to the problem of pion production in heavy-ion collision experiments has recently been given in [45]. Up to freeze-out, we consider the hydrodynamic description as relevant distribution $\rho_{\text{rel}}(t)$. With decreasing density, the relaxation to local thermodynamic equilibrium becomes less efficient, and the freeze-out time is determined by the condition that interaction processes are no longer able to sustain the local thermodynamic equilibrium. With respect to reactive collisions which change the particle numbers of the components, we denote this as chemical freeze-out. Elastic collisions remain possible at lower densities, they define the kine-

matic freeze-out. At freeze-out, one has to change the description of the non-equilibrium process because instead of the thermodynamic parameters more information is necessary to construct the relevant distribution, i.e. the concentration of the different components after chemical freeze out, or the single-particle distribution function after kinematic freeze-out. Then, the time evolution of the non-equilibrium system is described by reaction kinetics or kinetic equations.

Note that this transition from hydrodynamic to kinetic theory is not connected with a change of the physical process but only a question of the accuracy in the description if approximations are performed. At freeze-out the deviations from the local equilibrium or the relevant distribution become significant so that they have to be treated as new degrees of freedom. In practice, this change of the relevant description is performed assuming local thermodynamic equilibrium until freeze-out, and after that the reactions are described by the feed-down from excited states to the particles observed in the experiment. For a systematic non-equilibrium approach to nuclear processes see also [46].

In any case, an accurate description of the state of hot and dense matter in local thermodynamic equilibrium, i.e. $\rho_{\text{rel}}(t)$, is mandatory as prerequisite to formulate the non-equilibrium evolution of the system. Note that, in principle, $\rho_{\text{rel}}(t)$ has no influence on the final result if the limit $\epsilon \rightarrow 0$ is exactly performed. Missing correlations are produced dynamically solving the time evolution operator. However, in all calculations, approximations are indispensable, and a better choice of $\rho_{\text{rel}}(t)$ gives good results also in lowest approximation. Occupation numbers of single-particle states may be used to construct $\rho_{\text{rel}}(t)$ to describe the evolution after freeze-out. This leads to kinetic equations, but has problems to incorporate correlation effects. Therefore kinetic theory is not appropriate to describe the state of the system before freeze-out.

A second objection refers to the use of a simple statistical model, the hadron resonance gas (HRG), describing hot and dense matter in thermodynamic equilibrium as a mixture of non-interacting (with exception of reactive collisions) constituents. A better description should consider the effects of hadron-hadron interaction, and possible approaches are virial expansions known from nuclear physics [47, 48] which are related to the Beth-Uhlenbeck approach [49] as also shown in [50] neglecting in-medium corrections. The relativistic generalization is given by the S-matrix approach [51]. A particular problem is the treatment of correlations in the continuum which demands a systematic, quantum statistical approach. This approach has been successfully applied to solve the proton puzzle [52]. It was also applied to the strangeness enhancement [53]. We are interested in the application to further (composite) hadronic states where the yields are measured, in particular deuterons and antideuterons.

The experimental data we are interested in, are mainly central Pb-Pb collisions at LHC conditions. For instance, at collision energy $\sqrt{s_{NN}} = 2.76$ TeV, a fire-

ball is produced at midrapidity. At chemical freeze-out, it is characterized by the grand-canonical distribution $\rho_{\text{rel}}(t)$ with baryonic chemical potential $\mu_B \approx 0$, radius about 10.5 fm, corresponding to a volume of about 4200 fm³, and a temperature of about $T_{\text{fr}} = 156$ MeV. The number of measured charged pions per rapidity unit dN_{π}/dy ($dN_i/dy|_{y=0} = \int \frac{dp_T p_T}{(2\pi)^3} \sqrt{p_T^2 + m_i^2} e^{-\sqrt{p_T^2 + m_i^2}/T}$) is about 700, for all three species leading to roughly 2100, what corresponds to a pion density of about 0.34 fm⁻³. The fact that the baryo-chemical potential $\mu_B = 0$ requires that particles and antiparticles are produced with equal weight. It also means that the net-baryon density is zero. The numbers of protons/antiprotons and neutrons/antineutrons within this fireball are about 15 per species primordially, and close to 40 after taking into account the feed-down, each so that the baryon density is about 3×10^{-2} fm⁻³, i.e. very low. Whereas, in a first approach the hadronic resonance gas has proven to be surprisingly efficient to describe the observed yields, the new experiments give yields of different particles with high precision so that improvements of this simple model, in particular the effect of interactions, have to be taken into account to explain the data.

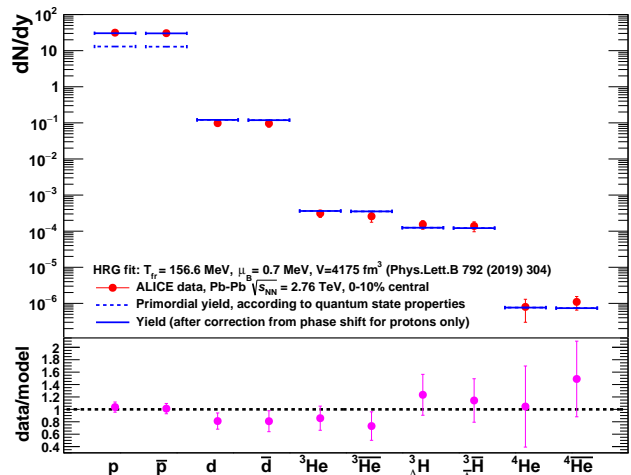


Figure 1. Result of the thermal model fit to ALICE data ($\sqrt{s_{NN}} = 2.76$ TeV, 0-10% central) on particles per rapidity unit dN/dy for non-strange (anti-)baryons and (anti-)(hyper-)nuclei using the S-matrix approach discussed below (for details of this fit see [52]). In detail, the figure shows in the upper panel the data (red) compared with the fit result, separated in primordial yield (dashed blue line) and final result (solid blue line) after feed-down and S-matrix correction for the protons. In addition, the data-over-model ratio is shown in the lower panel (in magenta), using the uncertainties of the data. One clearly sees that the protons and antiprotons are well described after the S-matrix correction. Whereas light nuclei are showing the same tension the protons showed before the correction (see [15]). Nevertheless, the uncertainties of light nuclei are still large enough to cope with the 1σ deviation, corresponding to 20-30% difference between fit and data.

The aim of this work is to investigate the modification of the yields of deuterons and antideuterons if a quantum statistical approach is used. Experimental data for the corresponding yields from the ALICE Collaboration at LHC are given in [52]. Figure I shows the experimental data on particles per rapidity unit dN/dy for non-strange (anti-)baryons and (anti-)(hyper-)nuclei measured by the ALICE Collaboration in Pb-Pb collisions at $\sqrt{s_{NN}} = 2.76$ TeV in a centrality interval of 0-10%, compared to the thermal model fit described in [52]. The fit using a hadronic resonance gas overestimates the measured deuteron and antideuteron yields by about 20%.

We consider improvements taking into account continuum correlations and interaction with the hot and dense surrounding matter. According to the composition given above, we expect that the main effects are caused by the pions, i.e. we have hadronic clusters embedded in hot and dense pionic matter. Consequently the main contribution to in-medium modification of hadrons is due to the interaction with pions, and the knowledge of corresponding scattering properties like phase shifts is necessary to calculate the in-medium effects on the composition. In our work, the partial density of deuteron-like correlations is investigated.

We start with the treatment of the interacting many-particle system and the introduction of partial densities in Sec. II. We give in Sec. III a short reference to the modification of the proton yield because of the interaction with surrounding pions as performed in Ref. [52]. In Sec. IV we discuss the formation of deuterons and the influence of continuum correlations, and in Sec. V we calculate the modification of the deuteron yield owing to the interaction with surrounding pions. Conclusions are drawn in Sec. VI.

II. PARTIAL INTRINSIC PARTITION FUNCTIONS

Hot and dense matter can't be described as ideal quantum gas. Because the components are interacting, correlations are formed. Examples are bound nuclei, in the ground state and excited states, but also resonances and continuum correlations. In this section, we demonstrate how the treatment of interactions for nuclear matter consisting of protons and neutrons allows to explain the formation of deuterons. We consider clusters of A nucleons which are characterized by total momentum P and further quantum numbers like isospin, here the proton number Z , and angular momentum J . Starting from a general quantum statistical approach, we decompose the total density in partial contributions from the different channels characterized by A, Z, J [54],

$$n_{\tau}^{\text{total}}(T, \mu_n, \mu_p) = \sum_{A, Z, J} A_{\tau} n_{A, Z, J}^{\text{part}}(T, \mu_n, \mu_p), \quad (2)$$

τ denotes neutron (n) or proton (p), and A_{τ} the neutron number ($A - Z$) or proton number (Z) of the cluster. The partial densities of the different channels are given by (non-degenerate case)

$$n_{A, Z, J}^{\text{part}}(T, \mu_n, \mu_p) = e^{((A-Z)\mu_n + Z\mu_p)/T} \times \int \frac{d^3P}{(2\pi)^3} e^{\frac{\hbar^2 P^2}{2Am_N T}} z_{A, Z, J}^{\text{part}}(P; T, \mu_n, \mu_p). \quad (3)$$

Am_N is the mass of the cluster $\{A, Z\}$ and m_N is the nucleon mass. Degeneracy effects are not relevant at conditions considered here, the Boltzmann probability distribution of the cluster states is given by the energy. After separation of the kinetic energy of the center-of-mass motion, the intrinsic partition function $z_{A, Z, J}^{\text{part}}$ contains all intrinsic excitations of the cluster.

We give the contributions of clusters with lowest mass number A . For $A = 1$ we have the contributions of free neutrons and protons, J is replaced by the spin direction, there are no intrinsic excitations within the hadronic phase at temperatures small compared to the energy of resonances so that the intrinsic partition function is $z_{A=1}^{\text{part}} = 1$. Within an advanced approach, the nucleon mass m_N should be replaced by the quasiparticle mass which contains the effect of a mean field. Well-known are, e.g., the relativistic mean-field approximations obtained from model Lagrangians which describes the coupling of the nucleons to mesonic fields, see for instance [55].

For $A = 2$ we have isospin triplet (nn, np, pp) channels as well as the isospin singlet (np) channel where the deuteron (d) is found as bound state. Therefore, this channel is of particular interest in our present work. The sum over the intrinsic excitations includes the continuum of scattering states. We replace the sum over the continuum states by the energy starting at the edge of continuum $E_d^{\text{cont}}(P)$ so that we have a generalized Beth-Uhlenbeck formula (degeneration factor 3 according spin 1)

$$z_d^{\text{part}}(P; T, \mu_n, \mu_p) = 3e^{-\frac{E_d^{\text{cont}}(P)}{T}} \left[\left(e^{B_d(P)/T} - 1 \right) \Theta[B_d(P)] + \frac{1}{\pi T} \int dE e^{-E/T} \left\{ \delta_d(E) - \frac{1}{2} \sin[2\delta_d(E)] \right\} \right]. \quad (4)$$

The edge of continuum $E_d^{\text{cont}}(P)$ is different from zero if quasiparticle energies are considered which modify the dispersion relation $\hbar^2 P^2 / (4m_N)$ for the center-of mass motion. $B_d(P)$ is the deuteron binding energy which in general is medium modified and thus depending on P as well as temperature T and chemical potentials of components, the same holds also for the scattering phase shifts $\delta_d(E)$. $\Theta[x]$ is the step function. The last term $\sin[2\delta_d(E)]$ is necessary to avoid double counting, because part of the interaction is already taken into account in the quasiparticle shifts of the nucleons [56]. In the limit of low densities, we can neglect the shift of the continuum edge and the medium modifications of bound state energies and scattering phase shifts. The treatment of the

second virial coefficient is given below in Sec. IV where the deuteron formation is considered.

III. PROTONS IN PION MATTER

The same approach can be generalized to other components of the many-body system. In this section, we are interested in the interaction of protons with pions as the main component in the fireball. The approach which has been worked out for interacting baryon systems will be applied here for a system mainly consisting of pions so that the interaction of nucleons with pions is the main effect. We present this issue here to compare with the work [52].

We briefly repeat the treatment of nucleons in pion matter. The hadron resonance gas would consider a mixture of pions, nucleons, Δ and other particles as listed, e.g., in the particle data book [57]. The primary yield ratio of all Δ resonances ($m_\Delta = 1232$ MeV) to nucleons ($m_N = 939$ MeV) is for $T_{\text{fr}} = 156$ MeV:

$$\frac{Y_\Delta^{\text{prim}}}{Y_n^{\text{prim}} + Y_p^{\text{prim}}} = \left(\frac{m_\Delta}{m_N}\right)^{3/2} \frac{16}{4} e^{-(m_\Delta - m_N)/T_{\text{fr}}} = 0.919. \quad (5)$$

These Δ resonances which are present in thermodynamic equilibrium at freeze-out, will disintegrate during the expansion of the hot and dense matter. Because baryon number is conserved, their decays feed into the nucleon and pion channels. Therefore, the final yields of the nucleon τ is increased compared to the primary yield by a factor of 1.919. In particular we expect within the hadron resonance gas model $Y_p^{\text{res.g.}\Delta} = 1.919 Y_p^{\text{prim}}$ only taking into account the contribution of the Δ resonances.

Additional resonances, in particular $N^*(1520)$, will also contribute. The HRG gives a factor 0.1498 in addition to the Δ resonances. The sum over all resonances given by the PDG [57] increases the final proton yield by the factor 2.743. This is shown in Fig. 2 where the primordial proton yield of 14.29 according to the temperature $T_{\text{fr}} = 156$ MeV is increased within the HRG model to 39.205 (including the feed-down from decays of primordial $\Delta(1232)$ with multiplicity 12.135 which is a substantial contribution).

However, this statistical hadronization model predicts about 25% more protons and antiprotons ($dN_p/dy = 39$ instead of 31) than measured by the ALICE Collaboration in central Pb-Pb collisions at the LHC. This constitutes the much debated proton-yield anomaly (also called proton "puzzle") in heavy-ion collisions at the LHC [52]. A possible approach to resolve this anomaly was to improve the non-interacting HRG model by using exact expressions for the second virial coefficient given by Dashen, Ma, and Bernstein [51] for the second virial coefficient, containing the pion-nucleon phase shifts.

We shortly repeat the calculation of the virial expansion of the density where the second virial coefficient is calculated within the Beth-Uhlenbeck approach [49]. In

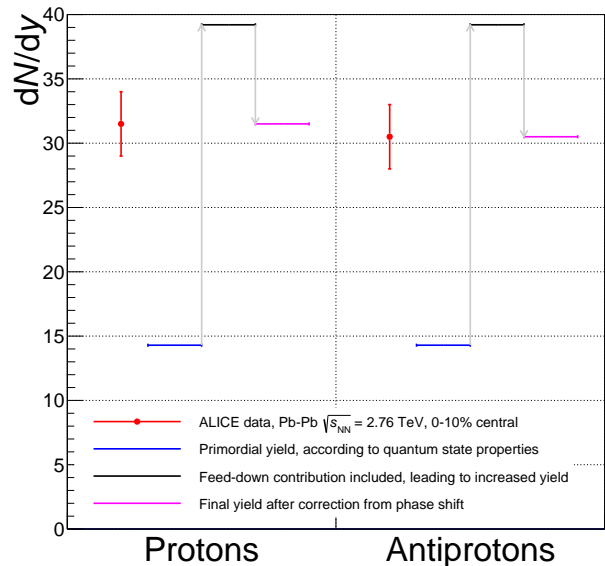


Figure 2. Comparison between experimental data from Pb-Pb collisions at $\sqrt{s_{\text{NN}}} = 2.76$ TeV for protons and antiprotons with values of model calculations. The red points indicate the production yield dN/dy and the vertical lines attached to them the quadratic sum of the statistical and systematic uncertainties. The blue horizontal lines indicate the primordial yields, the black lines the yields corrected for feed-down contributions and in magenta the yields corrected for the resonance contribution by the phase-shift analysis through the virial approach.

addition to the single-particle contributions describing the ideal gas of neutron and proton quasiparticles, the pion-nucleon channels are considered. They contain the Δ resonance seen in the P_{33} channel, as well as further excited states. The phase shifts for different channels are well known, fitted analytical expressions are available [58]. The intrinsic partition function $z_{A,Z,J}^{\text{part}}$ follows as

$$z_{1,Z,l}^{\text{part}} = \frac{1}{\pi T} \int \frac{d^3 p}{(2\pi)^3} \times \int \frac{dM}{2\pi} e^{-\sqrt{p^2 + M^2}/T} \left\{ \delta_l(M) - \frac{1}{2} \sin[2\delta_l(M)] \right\} \quad (6)$$

We use the generalized Beth-Uhlenbeck formula which accounts for the introduction of quasiparticles. The last term avoids double-counting because part of interaction (mean-field terms) is already included in the quasiparticle contribution. We use the free phase shifts to evaluate the expression and obtain the second virial coefficient. In-medium modifications of the scattering phase shifts [56] are not considered in this work.

The energy-dependent phase shifts of pion-nucleon

scattering below 400 MeV have been fitted in [58] as

$$\tan \delta_l = q^{2l+1} \left[b + cq^2 + dq^4 + \frac{x\Gamma_0\omega_0q_0^{-(2l+1)}}{\omega_0^2 - \omega^2} \right]. \quad (7)$$

(This fit is extended to energies larger than 400 MeV but gives only a contribution of few percent so that the error will be small. This is acceptable for this study, since we mainly want to show that the Beth-Uhlenbeck approach used here gives similar results as Dashen-Ma-Bernstein approach in Ref. [52]) For an exploratory calculation, we consider only the P_{33} channel which gives the dominant contribution. According to [58] we use for the P_{33} phase shift ($l = 1$) the values $b = 0.114/m_\pi^3$, $c = -0.0154/m_\pi^5$, $d = 0.00072/m_\pi^7$, $x = 0.99$, $\Gamma_0 = 116$, $\omega_0 = 1232$, $q_0 = 228$ (units MeV, MeV/c) and with m_π being the pion mass. For the freeze-out temperature $T_{\text{fr}} = 156$ MeV, we obtain using Eq. (6) for the proton using the pion-proton channel:

$$z_{1,1,1}^{\text{part}} = \frac{1}{\pi T} \int_0^\infty dE e^{-E/T_{\text{fr}}} \delta_1(E) = 0.388. \quad (8)$$

The account of the sin-term reduces this to 0.372 (about 5 %; note that phase shift must be given in radians).

Compared to the HRG result $e^{-(m_\Delta - m_N - m_\pi)/T_{\text{fr}}} = 0.374$ (note that the continuum edge contains also the pion mass $m_\pi = 139.6$ MeV) we have nearly the same result. With the multiplicity $4(m_\Delta/m_N)^{3/2}$ given in Eq. (5), we obtain the amount of Δ resonances which decay to nucleons when the hot matter is expanding after freeze-out. These feed-down processes contribute to the final proton yield.

However, other channels also contribute and we have to include higher resonances. A systematic calculation has been performed in [52]. We mainly wanted to show that our approach using the generalized Beth-Uhlenbeck formula works as well as the Dashen, Ma and Bernstein [51] approach. We will not repeat these calculations here but only present the main concepts to solve the proton puzzle. As a result, the reduction using the scattering phase shifts gives a total contribution of all proton-pion channels of 31.5 which feeds the final proton yield. The analogous calculation for antiprotons give the value 30.5, the small difference is due to the non vanishing, but small value of the baryonic chemical potential. The actual fit of the measured yields in Pb-Pb collisions at 2.76 TeV at the LHC leads to a value of $\mu_B = (0.7 \pm 3.8)$ MeV [15].

Figure 2 shows all involved steps to infer from the final experimental values for the yields of protons and antiprotons the primordial yields characterizing the composition at freeze-out. Feeding from the pion-proton channels, the primordial proton yield is changed to the final proton yield which is observed in experiments. The hadron resonance gas model predicts an enhancement of the primordial yield of the nucleons by a factor of 2.74 owing to the feed-down from hadronic resonances which is reduced to 2.204 using the virial approach, what agrees with the value seen from the final yields in the experiment.

IV. DEUTERON CHANNEL

We are interested in the deuteron production also observed in HIC. The number of measured deuterons per rapidity unit is $dN_d/dy = 0.098$ and $dN_{\bar{d}}/dy = 0.092$ for antideuterons. Within the simple approach of nuclear statistical equilibrium, the ratio of deuteron ($s = 1$) yield Y_d to proton ($s = 1/2$) yield Y_p is given as

$$R_{dp}^{\text{HRG}} = \frac{Y_d}{Y_p} = \frac{3}{2} \frac{\int d^3p/(2\pi)^3 e^{\sqrt{m_d^2 + p^2}/T}}{\int d^3p/(2\pi)^3 e^{\sqrt{m_p^2 + p^2}/T}} \quad (9)$$

assuming $\mu_B = 0$. With $T_{\text{fr}} = 156$ MeV the value $R_{dp}^{\text{HRG}} = 0.00874$ follows. Together with the value 14.29 for the proton yield given above, the deuteron yield is $dN_d^{\text{HRG}}/dy = 0.1249$, see also Fig. 3. Compared to the measured yields, the HRG model overestimates the deuteron production from HIC.

Several issues can be given which improve this simple statistical approach. As discussed at the beginning, the time evolution of the hot and dense matter produced in HIC collision is described by the statistical operator $\rho(t)$. This statistical operator $\rho(t)$ is formulated using the relevant statistical operator (Gibbs distribution) $\rho_{\text{rel}}(t')$

$$\rho_{\text{rel}} = \frac{e^{-\beta(H - \sum_i \mu_i N_i)}}{\text{Tr} e^{-\beta(H - \sum_i \mu_i N_i)}} \quad (10)$$

where H is the Hamiltonian of the system, N_i the particle number of conserved components i . In general, the Lagrange parameters β, μ_i , denoting the inverse temperature and the chemical potentials, are depending on position and time. In this context, the HRG Eq. (9) appears as a simple approximation where the Hamiltonian H is replaced by an expression where all interactions are neglected, after bound states have been introduced with the corresponding binding energies. An ideal, non-interacting mixture of free nucleons and bound states is considered, with accidental reactions and collisions to sustain partial equilibrium. We improve this in this work taking interactions into account as well as excited states, including continuum correlations.

A systematic quantum statistical approach introduces the spectral function which contains all correlations in the hot and dense nuclear matter. Two-particle correlations including the deuteron are obtained from the two-particle propagator, as solution of a Bethe-Salpeter equation. In contrast to the proton, the deuteron is a composite particle consisting of a neutron and a proton, with a binding energy $B_d = 2.225$ MeV. There are no excited bound states, but we have correlations in the continuum as described by the $n - p$ scattering phase shifts. As shown from the Beth-Uhlenbeck formula Eq. (4), the total amount of density in the deuteron channel is described by the second virial coefficient $b_{pn}(T)$,

$$n_d(T, \mu_n, \mu_p) = \frac{4}{\Lambda^3} e^{(\mu_n + \mu_p)/T} b_{pn}(T), \quad (11)$$

where $\Lambda = [2\pi/(m_N T)]^{1/2}$ is the thermal wave length of the nucleon, with mass m_N . An expression for the second virial coefficient including in-medium effects is obtained from the generalized Beth-Uhlenbeck formula [56] which can be used also in the high-density region.

Nevertheless, there are excited states of ${}^4\text{He}$, ${}^5\text{He}$ and ${}^5\text{Li}$ that are unstable particles (strong decays) and enhance the deuteron yield artificially [59]. These increase the (thermal) production yield by about 0.0225% as shown in Fig. 3. The feddown is such low since the penalty factor PF to produce one of the nuclei is about 330 per additional baryon [16]. For the higher mass nuclei mentioned above this means a suppression by PF^2 or even PF^3 , i.e. nearly negligible.

We consider the region of low baryon density where in-medium effects can be neglected. According to Beth and Uhlenbeck [49], the second virial coefficient can be expressed in terms of the binding energy and scattering phase shifts as

$$b_{pn}^{\text{vir}}(T) = \frac{3}{2^{1/2}} \left[e^{B_d/T} - 1 + \frac{1}{\pi T} \int_0^\infty dE e^{-E/T} \delta_{np}^{\text{total}}(E) \right]. \quad (12)$$

Here, E denotes the energy of relative motion, the energy of the center of mass motion of the two-nucleon system has been integrated over. Note that we use a nonrelativistic approach to introduce bound state wave functions and scattering phase shifts. Relativistic kinematics may be introduced, and the S-matrix approach can be given, but relativistic generalizations of statistical operator and in-medium Schrödinger equations demand much more effort.

Equation (4) and Eq. (12) can be given a compact form without subdivision of bound and scattering state contributions when a generalized scattering phase shift δ_d^{gen} is introduced, see [60, 61]. We define $\delta_d^{\text{gen}}(E, P) = \pi$ for $-|E_b(P)| \leq E \leq E_d^{\text{cont}}(P)$ if there exists a bound state with a binding energy $E_b(P)$, and $\delta_d^{\text{gen}}(E, P) = \delta(E, P)$ for $E \geq E_d^{\text{cont}}(P)$. For Eq. (4) we obtain:

$$z_d^{\text{part}}(P; T, \mu_n, \mu_p) = \frac{3}{\pi T} \int_{-\infty}^\infty dE e^{-E/T} \left\{ \delta_d^{\text{gen}}(E, P) - \frac{1}{2} \sin[2\delta_d^{\text{gen}}(E, P)] \right\}. \quad (13)$$

This expression represents the total amount of correlation, avoiding the (artificial) subdivision into a bound part contribution and a scattering part contribution. We note that for the bound state part of the generalized phase shift the contribution from the second term in the curly bracket vanishes because $\sin(2\pi)=0$.

Using the measured phase shifts, Horowitz and Schwenk [50] calculated values for $b_{pn}(T)$ for $1 \leq T \leq 20$ MeV. We followed these calculations and obtain for the freeze-out temperature $T_{\text{fr}} = 156$ MeV the value $b_{pn}(T_{\text{fr}}) = 0.887$. This means that the yield obtained from the HRG calculation is reduced by the factor

$$b_{pn}^{\text{vir}}(T_{\text{fr}}) \frac{2^{1/2}}{3} e^{-B_d/T_{\text{fr}}} = 0.412, \quad (14)$$

so that the production yield of deuterons

$$\frac{dN_d^{\text{virial}}}{dy} = 0.0514 \quad (15)$$

results. This value is shown in Fig. 3.

We conclude that the deuteron is only weakly bound, and considering the spectral function or the Beth-Uhlenbeck formula Eq. (12), most of the contribution to the correlated density in the isospin singlet channel, spin 1, is obtained from the continuum. The virial coefficient $b_{pn}^{\text{vir}}(T)$ contains all correlations in the isospin singlet channel where the deuteron is found as the state with lowest energy. Note that these deuteron-like correlations will not necessarily feed the observed deuteron states so that the calculated value dN_d^{virial}/dy represents an upper limit. Comparing with the simple nuclear statistical equilibrium yield $dN_d^{\text{HRG}}/dy = 0.1249$, a significant reduction of the deuteron yield is observed if continuum correlations are taken into account.

Like the production yield of protons calculated in the statistical model, the value dN_d^{virial}/dy is very small (about 1/2) compared to the measured yield $dN_d/dy = 0.098$. The yield of deuteron-like correlations in high-energy density matter according to the virial expansion shown in Fig. 3 underestimates the observed yield, similar to the primary proton yield shown in Fig. 2.

The question whether a weakly bound state such as the deuteron, $B_d = 2.225$ MeV can survive in a fireball with temperatures of the order 100 MeV, has been discussed in several publications, see for instance [62–65]. Like snowballs in hell, they argue that deuterons cannot survive in the fireball. According to the coalescence model, it is proposed that light nuclei are formed due to final-state interactions after the fireball decays. This means that chemical freeze-out up to which formation processes of deuterons are possible occur at a later instant of time, at different thermodynamic parameters. However, correlations are present also in matter with high density of energy at freeze-out, as described by quantum statistical approaches. The virial coefficient $b_{pn}(T_{\text{fr}}) = 0.887$ Eq. (14) expresses the amount of correlations for the interacting nucleon system at temperature T_{fr} .

The virial equation of state which accounts only for nucleon-nucleon interaction cannot explain the observed deuteron yields. Similar to the proton case, interaction with the pion system including the formation of resonances have to taken into account.

V. THE DEUTERON IN PION MATTER

Simple statistical models like the hadron resonance gas are improved when the interaction between the constituents is taken into account. Empirical approaches such as the concept of excluded volume (see for instance [66–68] and references therein) are not well founded. Before considering the interaction of the nucleons with pions, we shortly discuss the systematic treatment of the

interaction of deuterons with other nucleons. A quantum statistical approach has been worked out [56], and self-energy shifts and Pauli blocking effects have been investigated. The shift of the binding energy owing to Pauli blocking at nucleon density $n_p + n_n = 0.015 \text{ fm}^{-3}$ and $T_{fr} = 156 \text{ MeV}$ has been evaluated in [69] to be 0.2 MeV. This gives a reduction of about 1 per mille and can be neglected. Only at baryon densities of the order of the saturation density, $n_B \approx 0.1 \text{ fm}^{-3}$, medium effects become relevant.

However, we have a large value for the pion density so that the interaction with the pionic environment has to be considered, similar as done above for the case of protons. Before we perform a detailed calculation, we give a rough estimate along the lines of the hadron resonance gas (HRG). We focus on the Δ resonances which are dominant because of the low excitation energy and the large statistical factors (spin: 4, isospin: 4).

The deuteron is a weakly bound state of two nucleons which move almost freely. If we apply the impulse approximation, both constituents of the deuteron, at given distribution in momentum space according to the bound state wave function, are assumed to interact separately with the pion environment. We observe such a behavior in the pion-nucleon cross section [57] where the pion-deuteron scattering cross section is nearly the sum of the individual pion-nucleon cross sections. In particular, this refers also to the large peak near the position of the Δ resonances. Because nucleons in pionic matter are dressed forming resonances, we have also such resonances for the nucleons as constituents of the deuteron. If we assume that both nucleons forming the deuteron are dressed by pions so that single-nucleon spectral function has peaks near the hadronic resonances such as Δ , according to Eq. (5) an enhancement factor of $1.919^2 = 3.682$ would appear. Then, the production yield of deuterons would amount to

$$dN_d^{\text{res.gas}}/dy = 0.1892. \quad (16)$$

Here we assume that nucleon - Δ correlations behave similar to the nucleon-nucleon correlations which determine the virial expansion. As in the proton case, the Δ resonances decay after freeze-out to feed the nucleon yields.

Compared with the experimental yield, this estimate is very large already if no higher resonances are taken into account. It is obvious that such hadron resonance gas approximation is not realistic because we cannot expect that the proton-neutron interaction coincides with the corresponding baryon-baryon interaction including the Δ resonance to form the same correlations. The impulse approximation which neglects the energy dependence of the self-energy has to be improved.

To find a consistent solution, we should describe the deuteron in pion matter in a systematic way, as done above for the proton in pion matter to solve the proton puzzle.

A first-principle approach to describe the deuteron in

pion matter can be given considering the spectral function for the proton-neutron propagator in pion matter. As well known, the deuteron appears as a pole of this propagator in ladder approximation, solving the Bethe-Salpeter equation. The interaction with the pion environment is described by a self-energy, and a Beth-Uhlenbeck formula can be derived which expresses the density in terms of the deuteron-pion scattering phase shifts. We use the same approach as in the case of the proton in pion matter, replacing the proton, by the deuteron, both treated as elementary particles.

To include the interaction of the deuteron with the dense pion system produced by the HIC, we use the deuteron-pion scattering phase shifts. The Beth-Uhlenbeck formula is applied to the deuteron-pion channel and gives continuum correlations which may contribute to the observed deuteron yields. A phase-shift analysis of pion-deuteron scattering has been performed in Ref. [70–72], calculations for the total and integrated elastic cross sections are given in [73, 74], for a review of pion-deuteron scattering see [75]. The pion-deuteron scattering amplitude is presented by Argand plots. Of special interest is the p-wave amplitude calculated in different approximations [73, 75]. The amplitude f_{11}^2 for the partial-wave $f_{LL'}^J$ with a total momentum $J = 2$ and channel angular momentum $L, L' = 1$ is compared to experimental data in Ref. [70].

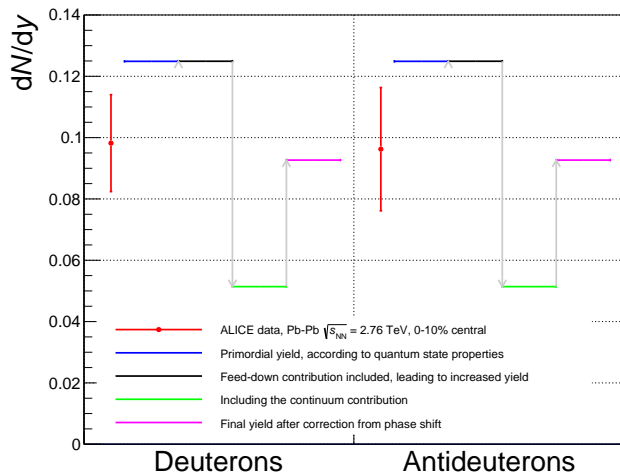


Figure 3. Comparison between experimental data from Pb-Pb collisions at $\sqrt{s_{NN}} = 2.76 \text{ TeV}$ for deuterons and antideuterons with model values. The red points indicate the production yield dN/dy and the vertical lines attached to them the quadratic sum of the statistical and systematic uncertainties. The blue horizontal lines indicate the primordial yields, the black lines the yields corrected for feed-down contributions, the green lines include the contribution from the continuum and the magenta lines the yields after correcting the resonance contribution by the phase-shift analysis through the Beth-Uhlenbeck approach.

The partial-wave pion-deuteron scattering amplitudes

$f_{LL'}^J$ are related to the strong phases $\delta_{LL'}^J$ and the S -matrix according to

$$S = 1 + 2ikf_{LL'}^J = e^{2i\delta_{LL'}^J} \quad (17)$$

where k is the momentum in the c.m. system. For exploratory calculations, we consider the amplitude f_{11}^2 which gives the largest contribution. The following fit has been performed to the Argand plots of Refs. [70, 73, 75] to the phase shifts here, E in MeV:

$$\tan \delta_{11}^2(E) = E^{3/2} \frac{13.5}{180^2 - E^2}. \quad (18)$$

The contribution of the pion-nucleon channel to the density is given by the intrinsic partition function, see Eq. (8)

$$z_{d,\pi,L=1} = \frac{1}{\pi T_{\text{fr}}} \int_0^\infty dE e^{-E/T_{\text{fr}}} \delta_{11}^2(E) = 0.312 \quad (19)$$

(note that the phase shift is in radians). With the degeneracy $g_\Delta = 16$, the shift of the continuum by the pion mass, and the center-of-mass motion we obtain the contribution of the pion-deuteron channel to the density

$$\begin{aligned} \frac{dN_d^{\text{total}}}{dy} &= 0.0514 \left[1 + 4 \left(\frac{2195.6}{1876} \right)^{3/2} e^{-m_\pi/T_{\text{fr}}} z_{d,\pi,L=1} \right] \\ &= 0.0927. \end{aligned} \quad (20)$$

This value is near to the experimental result, see Fig. 3. However, there are large uncertainties. Further pion-deuteron channels may be included, in particular f_{11}^1 and f_{22}^3 which will increase the deuteron-like density at freeze-out. But the contributions of the pion-deuteron scattering states may decay also to two nucleons as final states, considering the evolution of the fireball after freeze-out. For instance, the inelasticities of pion-deuteron collisions are also given in the Argand diagrams. They will not influence the chemical equilibrium as long as detailed balance holds. Thermodynamic equilibrium is not realized after freeze-out, because reactive collisions become rare. If they happen, a branching ratio of about 0.25 holds for elastic scattering [76], so 0.75 are inelastic break up reactions. This way, pion-deuteron collisions determine the feed down of deuteron contributions after freeze-out, which decay to nucleons. Nevertheless, this can be largely neglected as contribution to the nucleon yield since the deuteron yield at LHC is by the factor of about 300 suppressed compared to the nucleon yield [16]. The same argument can be used to explain that nucleon-nucleon (nn, pp, np) correlations are not essential for the proton yield, in contrast to the pion-proton correlations.

VI. CONCLUSIONS

It is obvious that a simple statistical model neglecting interaction effects cannot describe the composition of

the hot and dense system produced by HIC experiments adequately. However, this simple model with 2 or 3 parameters does a rather good job in describing the yields of most particles. Aiming at precision requires clearly corrections to the simple model. After the successful solution of the proton puzzle where the hadron-resonance gas overestimates the final proton yield, but the correct calculation of the scattering phase shifts gives the measured value, it was of interest to treat also other particles observed in the experiments. In the case of deuterons, the simple statistical model overestimates the deuteron yield seen in the experiment. The effect of pion-deuteron interaction in analogy to the hadron-resonance gas model would enhance the calculated deuteron yield because of feed-down from resonances like a $\Delta - N$ correlation, so that the discrepancy becomes larger. In the present work, before discussing the influence of the pion medium, we first explained that the deuteron yield is significantly reduced if the continuum correlations are included in accordance with the second virial coefficient. This is the main mechanism to reduce the deuteron yield.

Similar effects are also expected for the other nuclei like triton or ^4He . They are stronger bound, but the binding energy is also small compared to the temperature so that excited states and continuum correlations are relevant.

The most extreme example, displayed also in Fig. I and discussed intensively in [16, 17] is the hypertriton $^3_\Lambda\text{H}$, a bound state of a proton, a neutron and a Λ hyperon. The object can be imagined as a deuteron core surrounded by the Λ in form of a ultra-halo nucleus (size of about 10.8 fm [16, 77]). The hypertriton decays weakly and its lifetime is expected to be close to the one of the free Λ hyperon, since the Λ separation energy from the deuteron core is only about 130 keV and the probability to find the Λ far away from the core is high [78]. It would be outstanding to apply a phase shift correction as discussed here for the deuteron also to the hypertriton. Unfortunately is the data situation of scattering experiments for pions on the hypertriton even more scarce as for hyperons itself. Regrettably, the also here discussed impulse approximation approach did not lead to an acceptable result for the phase shift correction and therefore a different approach need to be found. It is also interesting to say that the correction needed would be in the opposite direction as the one for the deuteron and the ^3He as visible from Fig. I.

It should be mentioned that the concept of a deuteron as a weakly bound two-nucleon system in a hot environment looks strange, see [38, 62–65, 68, 79–82]. The rates of collisions to destroy or to form a nuclear bound state are large, but not of relevance in thermodynamic equilibrium because of detailed balance. We have a large contribution from continuum correlations, as described by the two-nucleon spectral function. These correlations in the deuteron channel are considered as precursors of the deuterons observed as the final deuteron yields. A similar concept is used in the coalescence model [17, 20–37]. Baryon pre-clusters are also discussed in [83–85] in

a slightly different approach.

As mentioned above, a more detailed description of the expansion process should consider also the fate of these correlations in the expanding system, for instance the evolution of the two-nucleon spectral function with time when the thermodynamic parameters of the environment of high-energy density change. The processes which define the final yields of mesons, nucleons and nuclei occur in the hadronic phase. Correlations freeze out when reaction rates become slow compared to the expansion rate. The question of freeze-out probes in heavy-ion collisions has been discussed also in context with strange hadron resonances [86]. Suppression of strange particle resonance production at LHC energies has been discussed recently [87–91]. Short-lived resonances, scattering and rescattering processes may help to achieve a better description of the expanding fireball after freeze-out. Feed-down concepts based on reaction networks are only approximations, a systematic treatment should be obtained from a non-equilibrium statistical operator approach.

The correct description of correlations in the relevant statistical operator, given up to freeze-out by the local thermodynamic equilibrium, is a prerequisite to describe the non-equilibrium evolution of the fireball produced by

heavy-ion collisions. Signatures of resonances, excited states, continuum correlations are also seen in the observed, final distribution of nucleons and nuclei.

ACKNOWLEDGEMENTS

We thank Johanna Stachel and Peter Braun-Munzinger for the hospitality and many useful discussions. We are also grateful to Volodymyr Vovchenko for helpful correspondence and for reading and commenting the paper draft. We also appreciate discussions with Volodymyr Vovchenko on the feed-down contribution of excited light nuclei. We further thank Anton Andronic and Pok Man Lo for the exchange about the S-matrix approach and the corresponding fit result.

This research was supported in part by the ExtreMe Matter Institute EMMI at the GSI Helmholtzzentrum für Schwerionenforschung, Darmstadt, Germany. B.D. acknowledges the support from Bundesministerium für Bildung und Forschung through ErUM-FSP T01 (Förderkennzeichen 05P21RFCA1). D.B. was supported by NCN under grant No. 2019/33/B/ST9/03059.

-
- [1] S. Acharya *et al.* (ALICE), Global baryon number conservation encoded in net-proton fluctuations measured in Pb-Pb collisions at $\sqrt{s_{NN}} = 2.76$ TeV, *Phys. Lett. B* **807**, 135564 (2020), arXiv:1910.14396 [nucl-ex].
- [2] S. Acharya *et al.* (ALICE), Relative particle yield fluctuations in Pb-Pb collisions at $\sqrt{s_{NN}} = 2.76$ TeV, *Eur. Phys. J. C* **79**, 236 (2019), arXiv:1712.07929 [nucl-ex].
- [3] S. Acharya *et al.* (ALICE), Neutral pion and η meson production at mid-rapidity in Pb-Pb collisions at $\sqrt{s_{NN}} = 2.76$ TeV, *Phys. Rev. C* **98**, 044901 (2018), arXiv:1803.05490 [nucl-ex].
- [4] S. Acharya *et al.* (ALICE), Production of ${}^4\text{He}$ and ${}^4\bar{\text{He}}$ in Pb-Pb collisions at $\sqrt{s_{NN}} = 2.76$ TeV at the LHC, *Nucl. Phys. A* **971**, 1 (2018), arXiv:1710.07531 [nucl-ex].
- [5] S. Acharya *et al.* (ALICE), Measurement of deuteron spectra and elliptic flow in Pb-Pb collisions at $\sqrt{s_{NN}} = 2.76$ TeV at the LHC, *Eur. Phys. J. C* **77**, 658 (2017), arXiv:1707.07304 [nucl-ex].
- [6] J. Adam *et al.* (ALICE), Centrality dependence of pion freeze-out radii in Pb-Pb collisions at $\sqrt{s_{NN}} = 2.76$ TeV, *Phys. Rev. C* **93**, 024905 (2016), arXiv:1507.06842 [nucl-ex].
- [7] J. Adam *et al.* (ALICE), ${}^3\text{H}$ and ${}^3\bar{\text{H}}$ production in Pb-Pb collisions at $\sqrt{s_{NN}} = 2.76$ TeV, *Phys. Lett. B* **754**, 360 (2016), arXiv:1506.08453 [nucl-ex].
- [8] J. Adam *et al.* (ALICE), Direct photon production in Pb-Pb collisions at $\sqrt{s_{NN}} = 2.76$ TeV, *Phys. Lett. B* **754**, 235 (2016), arXiv:1509.07324 [nucl-ex].
- [9] J. Adam *et al.* (ALICE), Production of light nuclei and anti-nuclei in pp and Pb-Pb collisions at energies available at the CERN Large Hadron Collider, *Phys. Rev. C* **93**, 024917 (2016), arXiv:1506.08951 [nucl-ex].
- [10] B. B. Abelev *et al.* (ALICE), Neutral pion production at midrapidity in pp and Pb-Pb collisions at $\sqrt{s_{NN}} = 2.76$ TeV, *Eur. Phys. J. C* **74**, 3108 (2014), arXiv:1405.3794 [nucl-ex].
- [11] B. B. Abelev *et al.* (ALICE), Multi-strange baryon production at mid-rapidity in Pb-Pb collisions at $\sqrt{s_{NN}} = 2.76$ TeV, *Phys. Lett. B* **728**, 216 (2014), [Erratum: *Phys. Lett. B* 734, 409–410 (2014)], arXiv:1307.5543 [nucl-ex].
- [12] B. B. Abelev *et al.* (ALICE), K_S^0 and Λ production in Pb-Pb collisions at $\sqrt{s_{NN}} = 2.76$ TeV, *Phys. Rev. Lett.* **111**, 222301 (2013), arXiv:1307.5530 [nucl-ex].
- [13] B. Abelev *et al.* (ALICE), Centrality dependence of π , K, p production in Pb-Pb collisions at $\sqrt{s_{NN}} = 2.76$ TeV, *Phys. Rev. C* **88**, 044910 (2013), arXiv:1303.0737 [hep-ex].
- [14] B. Abelev *et al.* (ALICE), Pion, Kaon, and Proton Production in Central Pb-Pb Collisions at $\sqrt{s_{NN}} = 2.76$ TeV, *Phys. Rev. Lett.* **109**, 252301 (2012), arXiv:1208.1974 [hep-ex].
- [15] A. Andronic, P. Braun-Munzinger, K. Redlich, and J. Stachel, Decoding the phase structure of QCD via particle production at high energy, *Nature* **561**, 321 (2018), arXiv:1710.09425 [nucl-th].
- [16] P. Braun-Munzinger and B. Dönigus, Loosely-bound objects produced in nuclear collisions at the LHC, *Nucl. Phys. A* **987**, 144 (2019), arXiv:1809.04681 [nucl-ex].
- [17] B. Dönigus, Selected highlights of the production of light (anti-)(hyper-)nuclei in ultra-relativistic heavy-ion collisions, *Eur. Phys. J. A* **56**, 280 (2020).
- [18] P. Braun-Munzinger, K. Redlich, and J. Stachel, *Particle production in heavy ion collisions, invited review in: R.C. Hwa, X.N. Wang Eds., Quark Gluon Plasma, vol. 3* (World Scientific Publishing, 2003) arXiv:nucl-

- th/0304013.
- [19] B. Dönigus, Light nuclei in the hadron resonance gas, *Int. J. Mod. Phys. E* **29**, 2040001 (2020), arXiv:2004.10544 [nucl-th].
- [20] L. P. Csernai and J. I. Kapusta, Entropy and Cluster Production in Nuclear Collisions, *Phys. Rept.* **131**, 223 (1986).
- [21] R. Mattiello, A. Jahns, H. Sorge, H. Stoecker, and W. Greiner, Deuteron flow in ultrarelativistic heavy ion reactions, *Phys. Rev. Lett.* **74**, 2180 (1995).
- [22] M. Bleicher, C. Spieles, A. Jahns, R. Mattiello, H. Sorge, H. Stoecker, and W. Greiner, Phase space correlations of anti-deuterons in heavy ion collisions, *Phys. Lett. B* **361**, 10 (1995), arXiv:nucl-th/9506009.
- [23] J. L. Nagle, B. S. Kumar, D. Kusnezov, H. Sorge, and R. Mattiello, Coalescence of deuterons in relativistic heavy ion collisions, *Phys. Rev. C* **53**, 367 (1996).
- [24] R. Scheibl and U. W. Heinz, Coalescence and flow in ultrarelativistic heavy ion collisions, *Phys. Rev. C* **59**, 1585 (1999), arXiv:nucl-th/9809092.
- [25] J. Steinheimer *et al.*, Hypernuclei, dibaryon and antinuclei production in high energy heavy ion collisions: Thermal production versus Coalescence, *Phys. Lett. B* **714**, 85 (2012), arXiv:1203.2547 [nucl-th].
- [26] K.-J. Sun and L.-W. Chen, Production of antimatter ${}^{5,6}\text{Li}$ nuclei in central Au+Au collisions at $\sqrt{s_{NN}} = 200$ GeV, *Phys. Lett. B* **751**, 272 (2015), arXiv:1509.05302 [nucl-th].
- [27] K.-J. Sun and L.-W. Chen, Antimatter ${}^4\text{H}$ Hypernucleus Production and the ${}^3\text{H}/{}^3\text{He}$ Puzzle in Relativistic Heavy-Ion Collisions, *Phys. Rev. C* **93**, 064909 (2016), arXiv:1512.00692 [nucl-th].
- [28] A. S. Botvina, J. Steinheimer, and M. Bleicher, Formation of exotic baryon clusters in ultrarelativistic heavy-ion collisions, *Phys. Rev. C* **96**, 014913 (2017), arXiv:1706.08335 [nucl-th].
- [29] F. Bellini and A. P. Kalweit, Testing production scenarios for (anti-)(hyper-)nuclei and exotica at energies available at the CERN Large Hadron Collider, *Phys. Rev. C* **99**, 054905 (2019), arXiv:1807.05894 [hep-ph].
- [30] S. Sombun, K. Tomuang, A. Limphirat, P. Hillmann, C. Herold, J. Steinheimer, Y. Yan, and M. Bleicher, Deuteron production from phase-space coalescence in the UrQMD approach, *Phys. Rev. C* **99**, 014901 (2019), arXiv:1805.11509 [nucl-th].
- [31] W. Zhao, L. Zhu, H. Zheng, C. M. Ko, and H. Song, Spectra and flow of light nuclei in relativistic heavy ion collisions at energies available at the BNL Relativistic Heavy Ion Collider and at the CERN Large Hadron Collider, *Phys. Rev. C* **98**, 054905 (2018), arXiv:1807.02813 [nucl-th].
- [32] K.-J. Sun, C. M. Ko, and B. Dönigus, Suppression of light nuclei production in collisions of small systems at the Large Hadron Collider, *Phys. Lett. B* **792**, 132 (2019), arXiv:1812.05175 [nucl-th].
- [33] M. Kachelrieß, S. Ostapchenko, and J. Tjemsland, Alternative coalescence model for deuteron, tritium, helium-3 and their antinuclei, *Eur. Phys. J. A* **56**, 4 (2020), arXiv:1905.01192 [hep-ph].
- [34] K.-J. Sun and C. M. Ko, Light nuclei production in a multiphase transport model for relativistic heavy ion collisions, *Phys. Rev. C* **103**, 064909 (2021), arXiv:2005.00182 [nucl-th].
- [35] P. Hillmann, K. Käfer, J. Steinheimer, V. Vovchenko, and M. Bleicher, Coalescence, the thermal model and multi-fragmentation: the energy and volume dependence of light nuclei production in heavy ion collisions, *J. Phys. G* **49**, 055107 (2022), arXiv:2109.05972 [hep-ph].
- [36] S. Gläsel *et al.*, Cluster and hypercluster production in relativistic heavy-ion collisions within the parton-hadron-quantum-molecular-dynamics approach, *Phys. Rev. C* **105**, 014908 (2022), arXiv:2106.14839 [nucl-th].
- [37] W. Zhao, K.-J. Sun, C. M. Ko, and X. Luo, Multiplicity scaling of light nuclei production in relativistic heavy-ion collisions, *Phys. Lett. B* **820**, 136571 (2021), arXiv:2105.14204 [nucl-th].
- [38] P. Braun-Munzinger and J. Stachel, Production of strange clusters and strange matter in nucleus-nucleus collisions at the AGS, *J. Phys. G* **21**, L17 (1995), arXiv:nucl-th/9412035.
- [39] J. Cleymans, S. Kabana, I. Kraus, H. Oeschler, K. Redlich, *et al.*, Antimatter production in proton-proton and heavy-ion collisions at ultrarelativistic energies, *Phys. Rev. C* **84**, 054916 (2011), arXiv:1105.3719 [hep-ph].
- [40] A. S. Botvina and I. N. Mishustin, Statistical approach for supernova matter, *Nucl. Phys. A* **843**, 98 (2010), arXiv:0811.2593 [nucl-th].
- [41] N. Buyukcizmeci *et al.*, A comparative study of statistical models for nuclear equation of state of stellar matter, *Nucl. Phys. A* **907**, 13 (2013), arXiv:1211.5990 [nucl-th].
- [42] M. Floris, Hadron yields and the phase diagram of strongly interacting matter, *Nuclear Physics A* **931**, 103 (2014).
- [43] V. Vovchenko, B. Dönigus, and H. Stoecker, Multiplicity dependence of light nuclei production at LHC energies in the canonical statistical model, *Phys. Lett. B* **785**, 171 (2018), arXiv:1808.05245 [hep-ph].
- [44] D. Zubarev *et al.*, *Statistical Mechanics of Non-equilibrium Processes* (Wiley, 1996/1997).
- [45] D. Blaschke, G. Röpke, D. N. Voskresensky, and V. G. Morozov, Nonequilibrium pion distribution within the Zubarev approach, *Particles* **3**, 380 (2020), arXiv:2004.05401 [hep-ph].
- [46] G. Röpke, J. B. Natowitz, and H. Pais, Nonequilibrium information entropy approach to ternary fission of actinides, *Phys. Rev. C* **103**, 061601 (2021), arXiv:2012.14691 [nucl-th].
- [47] G. Röpke, L. Münchow, and H. Schulz, Particle clustering and Mott transitions in nuclear matter at finite temperature, *Nucl. Phys. A* **379**, 536 (1982).
- [48] G. Röpke, L. Münchow, and H. Schulz, On the phase stability of hot nuclear matter and the applicability of detailed balance equations, *Phys. Lett. B* **110**, 21 (1982).
- [49] E. Beth and G. Uhlenbeck, The quantum theory of the non-ideal gas. II. Behaviour at low temperatures, *Physica* **4**, 915 (1937).
- [50] C. J. Horowitz and A. Schwenk, Cluster formation and the virial equation of state of low-density nuclear matter, *Nucl. Phys. A* **776**, 55 (2006), arXiv:nucl-th/0507033.
- [51] R. Dashen, S.-K. Ma, and H. J. Bernstein, S Matrix formulation of statistical mechanics, *Phys. Rev.* **187**, 345 (1969).
- [52] A. Andronic, P. Braun-Munzinger, B. Friman, P. M. Lo, K. Redlich, and J. Stachel, The thermal proton yield anomaly in Pb-Pb collisions at the LHC and its resolution, *Phys. Lett. B* **792**, 304 (2019), arXiv:1808.03102 [hep-ph].

- [53] J. Cleymans, P. M. Lo, K. Redlich, and N. Sharma, Multiplicity dependence of (multi)strange baryons in the canonical ensemble with phase shift corrections, *Phys. Rev. C* **103**, 014904 (2021), arXiv:2009.04844 [hep-ph].
- [54] G. Röpke, Nuclear matter equation of state including two-, three-, and four-nucleon correlations, *Phys. Rev. C* **92**, 054001 (2015), arXiv:1411.4593 [nucl-th].
- [55] S. Typel, G. Röpke, T. Klähn, D. Blaschke, and H. H. Wolter, Composition and thermodynamics of nuclear matter with light clusters, *Phys. Rev. C* **81**, 015803 (2010), arXiv:0908.2344 [nucl-th].
- [56] M. Schmidt, G. Röpke, and H. Schulz, Generalized Beth-Uhlenbeck approach for hot nuclear matter, *Annals Phys.* **202**, 57 (1990).
- [57] P. Zyla *et al.* (Particle Data Group), Review of Particle Physics, *PTEP* **2020**, 083C01 (2020), and 2021 update.
- [58] G. Rowe, M. Salomon, and R. H. Landau, An Energy Dependent Phase Shift Analysis of Pion - Nucleon Scattering Below 400-MeV, *Phys. Rev. C* **18**, 584 (1978).
- [59] V. Vovchenko, B. Dönigus, B. Kardan, M. Lorenz, and H. Stoecker, Feeddown contributions from unstable nuclei in relativistic heavy-ion collisions, *Phys. Lett. B*, 135746 (2020), arXiv:2004.04411 [nucl-th].
- [60] G. Röpke, Clustering in nuclear environment, *J. Phys. Conf. Ser.* **569**, 012031 (2014), arXiv:1408.2654 [nucl-th].
- [61] N.-U. F. Bastian, D. Blaschke, T. Fischer, and G. Röpke, Towards a Unified Quark-Hadron Matter Equation of State for Applications in Astrophysics and Heavy-Ion Collisions, *Universe* **4**, 67 (2018), arXiv:1804.10178 [nucl-th].
- [62] S. Mrowczynski, Production of light nuclei in the thermal and coalescence models, *Acta Phys. Polon. B* **48**, 707 (2017), arXiv:1607.02267 [nucl-th].
- [63] D. Oliinychenko, L.-G. Pang, H. Elfner, and V. Koch, Microscopic study of deuteron production in PbPb collisions at $\sqrt{s} = 2.76\text{TeV}$ via hydrodynamics and a hadronic afterburner, *Phys. Rev. C* **99**, 044907 (2019), arXiv:1809.03071 [hep-ph].
- [64] V. Vovchenko, K. Gallmeister, J. Schaffner-Bielich, and C. Greiner, Nucleosynthesis in heavy-ion collisions at the LHC via the Saha equation, *Phys. Lett. B* **800**, 135131 (2020), arXiv:1903.10024 [hep-ph].
- [65] S. Mrowczynski, Production of light nuclei at colliders – coalescence vs. thermal model, *Eur. Phys. J. ST* **229**, 3559 (2020), arXiv:2004.07029 [nucl-th].
- [66] M. Hempel and J. Schaffner-Bielich, Statistical Model for a Complete Supernova Equation of State, *Nucl. Phys. A* **837**, 210 (2010), arXiv:0911.4073 [nucl-th].
- [67] V. Vovchenko, Hadron resonance gas with van der Waals interactions, *Int. J. Mod. Phys. E* **29**, 2040002 (2020), arXiv:2004.06331 [nucl-th].
- [68] K. A. Bugaev *et al.*, Second virial coefficients of light nuclear clusters and their chemical freeze-out in nuclear collisions, *Eur. Phys. J. A* **56**, 293 (2020), arXiv:2005.01555 [nucl-th].
- [69] G. Röpke, Light nuclei quasiparticle energy shift in hot and dense nuclear matter, *Phys. Rev. C* **79**, 014002 (2009), arXiv:0810.4645 [nucl-th].
- [70] J. Arvieux and A. S. Rinat, A Phase Shift Analysis of Elastic Pion - Deuteron Scattering, *Nucl. Phys. A* **350**, 205 (1980).
- [71] A. S. Rinat and Y. Starkand, A Comparative Study of the $NN\pi$ System. 1. The $\pi d \rightarrow \pi d$, $\pi d \rightarrow NN$ Channels, *Nucl. Phys. A* **397**, 381 (1983).
- [72] H. Garcilazo *et al.*, Polarization Observables in πD (Polarized) Elastic Scattering: Amplitude Analysis, *Phys. Rev. C* **39**, 942 (1989).
- [73] R. M. Woloshyn, E. J. Moniz, and R. Aaron, Relativistic Three-Body Calculation of π -d Scattering, *Phys. Rev. C* **13**, 286 (1976).
- [74] N. Hiroshige, W. Watari, and M. Yonezawa, Pion - Deuteron Elastic Scattering Amplitudes in $T(\pi, L) = 117\text{-MeV}$ to 325-MeV Region, *Prog. Theor. Phys.* **72**, 1282 (1984).
- [75] A. W. Thomas and R. H. Landau, Pion - Deuteron and Pion - Nucleus Scattering: A Review, *Phys. Rept.* **58**, 121 (1980).
- [76] J. H. Norem, Interactions of 290 MeV/c positive pions with deuterium, *Nucl. Phys. B* **33**, 512 (1971).
- [77] F. Hildenbrand and H.-W. Hammer, Three-Body Hypernuclei in Pionless Effective Field Theory, *Phys. Rev. C* **100**, 034002 (2019), arXiv:1904.05818 [nucl-th].
- [78] A. Gal, E. V. Hungerford, and D. J. Millener, Strangeness in nuclear physics, *Rev. Mod. Phys.* **88**, 035004 (2016), arXiv:1605.00557 [nucl-th].
- [79] P. Braun-Munzinger, B. Dönigus and N. Löhner, ALICE investigates 'snowballs in hell', *CERN Courier* **September**, 26 (2015).
- [80] K. Gallmeister and C. Greiner, Production of light nuclei in heavy ion collisions via hagedorn resonances, *Eur. Phys. J. A* **57**, 62 (2021), arXiv:2007.08258 [hep-ph].
- [81] T. Neidig, K. Gallmeister, C. Greiner, M. Bleicher, and V. Vovchenko, Towards solving the puzzle of high temperature light (anti)-nuclei production in ultra-relativistic heavy ion collisions, *Phys. Lett. B* **827**, 136891 (2022), arXiv:2108.13151 [hep-ph].
- [82] K.-J. Sun, R. Wang, C. M. Ko, Y.-G. Ma, and C. Shen, Relativistic kinetic approach to light nuclei production in high-energy nuclear collisions (2021), arXiv:2106.12742 [nucl-th].
- [83] E. Shuryak and J. M. Torres-Rincon, Baryon clustering at the critical line and near the hypothetical critical point in heavy-ion collisions, *Phys. Rev. C* **100**, 024903 (2019), arXiv:1805.04444 [hep-ph].
- [84] E. Shuryak and J. M. Torres-Rincon, Baryon preclustering at the freeze-out of heavy-ion collisions and light-nuclei production, *Phys. Rev. C* **101**, 034914 (2020), arXiv:1910.08119 [nucl-th].
- [85] E. Shuryak and J. M. Torres-Rincon, Light-nuclei production and search for the QCD critical point, *Eur. Phys. J. A* **56**, 241 (2020), arXiv:2005.14216 [nucl-th].
- [86] C. Markert, G. Torrieri, and J. Rafelski, Strange Hadron Resonances: Freeze-Out Probes in Heavy-Ion Collisions, *AIP Conf. Proc.* **631**, 533 (2002), arXiv:hep-ph/0206260.
- [87] S. Acharya *et al.* (ALICE), Suppression of $\Lambda(1520)$ resonance production in central Pb-Pb collisions at $\sqrt{s_{NN}} = 2.76\text{ TeV}$, *Phys. Rev. C* **99**, 024905 (2019), arXiv:1805.04361 [nucl-ex].
- [88] A. Motornenko, V. Vovchenko, C. Greiner, and H. Stoecker, Kinetic freeze-out temperature from yields of short-lived resonances, *Phys. Rev. C* **102**, 024909 (2020), arXiv:1908.11730 [hep-ph].
- [89] S. Acharya *et al.* (ALICE), Pion-kaon femtoscopy and the lifetime of the hadronic phase in Pb-Pb collisions at $\sqrt{s_{NN}} = 2.76\text{ TeV}$, *Phys. Lett. B* **813**, 136030 (2021), arXiv:2007.08315 [nucl-ex].
- [90] S. Acharya *et al.* (ALICE), Production of light (anti)nuclei in pp collisions at $\sqrt{s} = 5.02\text{ TeV}$, *Eur. Phys.*

J. C **82**, 289 (2022), arXiv:2112.00610 [nucl-ex].
[91] A. G. Knospe, C. Markert, K. Werner, J. Steinheimer,
and M. Bleicher, Hadronic resonance production and in-
teraction in p-Pb collisions at LHC energies in EPOS3,

Phys. Rev. C **104**, 054907 (2021), arXiv:2102.06797
[nucl-th].